Submitted June 2007

Detection and Classification of Weld Discontinuities in Radiographic Images (Part II: Unsupervised Learning)

by Germano X. de Pádua,* Romeu R. da Silva,† Domingo Mery,‡ João M.A. Rebello§ and Luiz P. Calôba**

ABSTRACT

The importance of industrial radiography as a nondestructive testing method is unquestionable and has lasted more than half a century. This paper presents innovative non-supervised pattern recognition application methodologies, evaluating the formation of cross-sectional profile patterns of grays corresponding to typical welding discontinuities extracted from radiographic images. The techniques involve the development of networks of the modified adaptive resonance theory (ART) type as well as the phenomenologic study of the patterns of each class of discontinuity. The results obtained are pioneering in this kind of research and are quite promising, mainly in connection with the image processing techniques that aim to extract data from the radiographic weld bead and in the detection and classification of discontinuities by analyzing the cross-sectional profile of the gray level. This is the second of three articles describing the work done on using these profiles as inputs for the classifiers.

Keywords: *transversal gray level profiles, adaptive resonance theory, weld discontinuities, radiography, nondestructive testing.*

INTRODUCTION

Industrial radiography (Halmshaw, 1995) is a nondestructive testing method with wide application in various industries, especially in the petroleum industry. Because it involves visual analysis of images, the conventional technique is subject to interpretation errors by the operator (Fücsök and Scharmach, 2000; Fücsök et al., 2002). For that reason, the development of computers, image processing techniques and pattern recognition systems (Duda et al., 2001; Haykin, 1994) has received much attention, with considerable work being done on the development of a system for the digital interpretation of radiographs, with radiographs of welds (da Silva et al., 2001; da Silva et al., 2002; da Silva et al., 2004; da Silva et al., 2005; da Silva and Mery, 2007a; da Silva and Mery, 2007b) and castings (Mery, 2006) clearly standing out.

Among several lines of research for the development of an automatic or semiautomatic system for detecting welding discontinuities in radiographic images, there is one line that deals with the use of transverse profiles of gray levels in the weld bead as relevant information for the detection and even the classification of welding discontinuities (Liao and Li, 1998; Liao and Ni, 1996; Liao et al., 1999; de Pádua et al., 2004).

This paper presents methodologies and results referring to research done for finding patterns representative of transverse profiles of gray levels in weld beads, with the main purpose of contributing to the research lines in this field and providing a tool that can help in case of doubt of the classes of welding discontinuities. For that purpose, radiographic images of discontinuity patterns manufactured by the International Institute of Welding and the Federal Institute for Materials Research and Testing, Berlin were used.

This work can be connected to the research of various authors such as Liao and Ni (1996), Liao and Li (1998) and Felisberto et al. (2006).

It is important to point out that, even though there are many books on this matter (Haykin, 1994; Wasserman, 1989), a short description will be made of adaptive resonance theory (ART) networks, and mainly of the modifications made to it because it is not a methodology used much in this field of research, and that might hinder the correct interpretation of the results obtained by researchers who are not well acquainted with it.

METHODOLOGIES

Radiographic Films

The digital radiographic images used in this work are the same as those in Part I of this paper (published in the November issue of this journal), and therefore their descriptions are not given again.

Unsupervised Networks

Besides supervised learning, neural networks are also capable of receiving unsupervised or semisupervised learning (Haykin, 1994). Besides classifying the events, this kind of learning allows the user to obtain the class patterns. Modified ART neural networks have been used to obtain the patterns of each class and also as classifiers for comparing with the results of supervised networks (Part I).

An unsupervised network is that in which knowing the desired output is not necessary for the network to adapt and produce the expected response. Classifiers developed by similarity, in the case of this work, particularly those developed by neural networks, have interesting properties, some of which are very useful:

- training is usually much faster than with supervised training
- the network can be trained and operated simultaneously (though performance in the operation depends on the amount of training already done)
- every class is trained in a reasonably independent way from the rest (this returns to the plastic network: existing classes can be altered or removed, the same as new classes introduced, without altering the performance of the other classes already "learned," an important characteristic for this work)
- its architecture is simple and open, allowing easy hybridization with other networks and concepts, as in this work (it allows an easy geometric interpretation of the modus operandi of the classifier, as opposed to the feed-forward network trained by error backpropagation)
- the network generates "patterns" for the classes, allowing the knowledge of the phenomenology of the case to be extended.

Consider a case in which this problem can be fitted, where every input $\mathbf{x}$ can be seen as a pattern $\mathbf{w}$ to which a noise $\mathbf{r}$ was added: $\mathbf{x} = \mathbf{w} + \mathbf{r}$. Assuming that the noise is a gaussian blank, that is, the noise

* Petróleo Brasileiro SA – Petrobras, 81 Alm. Barroso Av. 27th floor, Rio de Janeiro, RJ, Brazil; e-mail <germanox@petrobras.com.br>.
† Departamento de Ciencia de la Computación, Pontificia Universidad Católica de Chile.
‡ Departamento de Ciencia de la Computación, Pontificia Universidad Católica de Chile; e-mail <dmery@ing.puc.cl>.
§ Department of Metallurgical and Materials Engineering, Federal University of Rio de Janeiro (UFRJ), PO Box 68505, CEP 21945-970, Rio de Janeiro, RJ, Brazil.
** Department of Electrical Engineering, Federal University of Rio de Janeiro (UFRJ), PO Box 68504, CEP 21945-970, Rio de Janeiro, RJ, Brazil.

of each component of $\mathbf{r}$ has a null mean, the same variance σ^2, a gaussian distribution, and they are not correlated, the inputs $\mathbf{x}$ will be distributed in a hypersphere centered on $\mathbf{w}$. Without losing generality and to facilitate visualization, let us consider $\mathbf{x}$ to be bidimensional and $|\mathbf{x}| \neq 1$ (just for visualization). Figure 1a shows the domain of different classes with different noise and with overlapping regions.

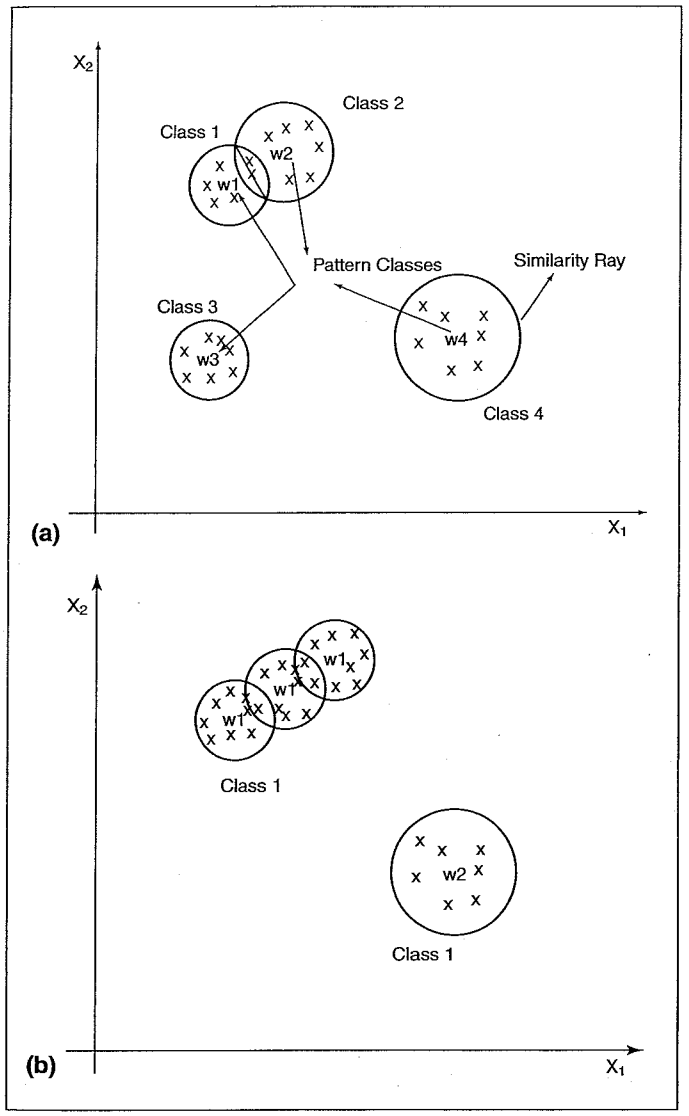

Figure 1 — Class representations: (a) a vector classification according to four patterns and spheres of similarity; (b) a nonspherical (C_1) and spherical (C_2) class distribution.

There are cases in which the class can be better represented by more than one pattern, thereby losing its spherical characteristic. In that case, several spheres (patterns) can be used to represent this class, as shown in Figure 1b.

These kinds of data suggest that the domain of the classes is bounded by hyperspheres. For clustering to be successful, it is essential to choose the radius of the hypersphere of each class properly; hyperspheres with radii that are too large set limits to the domain much larger than those of the class and can enclose inputs that belong to other classes of defects (rejectable discontinuities); radii that are too small will require a large number of patterns to represent a class.

The distribution of the distances d_i of the inputs $\mathbf{x}_i$ to the corresponding patterns $\mathbf{w}$ is a distribution of $|\mathbf{r}|$. It is the positive side of a gaussian with variance $n\sigma^2$, where n is the dimension of $\mathbf{x}$ and σ^2 is the variance of each of its components. Figure 2 outlines the shape of this distribution with a solid line.

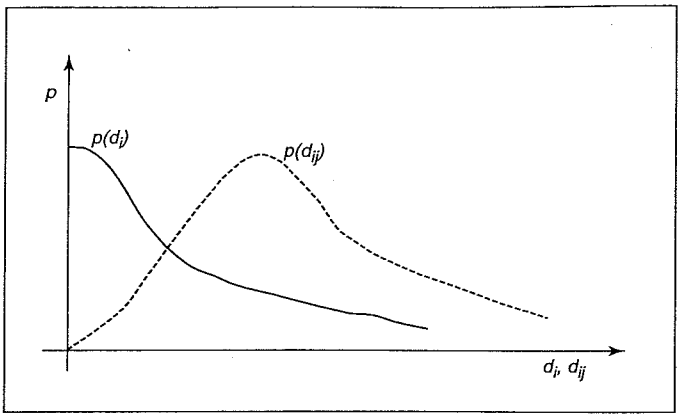

Figure 2 — Distribution scheme of $p(d_i)$ *and* $p(d_{ij})$.

Considering the $p(d_{ij})$ distribution normal (with d_{ij} the distance between each input), a reasonable value for the radius of the hyperesphere (similarity) that contains this class is:

$$r \cong 2.5\sqrt{n\sigma} \tag{1}$$

where

the constant 2.5 statistically includes 90% of the samples.

Usually, it is not practical to calculate this value in more complex classes with various patterns (for example, class 1 of Figure 1b).

The distribution of the distances d_{ij} between the two inputs $\mathbf{x}_i$ and $\mathbf{x}_j$ associated with the same pattern $\mathbf{w}$ corresponds to a distribution, according to the scheme of Figure 2, with a mean (and mode, approximately) equal to:

$$m \cong \sqrt{2n\sigma} \tag{2}$$

In the case of a complex class with several patterns $\mathbf{w}$, m can be identified as the smallest mode of the distribution of d_{ij} and can be determined easily. If we consider that the smallest diameter of a class is equal to or greater than the diameter of the hyperspheres that determine its domain, then from Equations 1 and 2 we obtain:

$$r \cong \frac{2.5}{\sqrt{2}} m \cong 1.5m \tag{3}$$

where

r = the largest radius of similarity recommended for each class.

Equations and Structure of the Modified ART Network

Considering what was described above, in the case of several classes C_i with different patterns $\mathbf{w}_i$, the most probable class for an input $\mathbf{x}$ formed by a pattern corrupted by white noise is that whose pattern $\mathbf{w}$ is most similar to input $\mathbf{x}$, that is,

$$x \in C_i \Leftrightarrow s_i > s_j \forall j \neq i \tag{4}$$

where

$$s_i = \mathbf{x}^t \mathbf{w}_i; \ |\mathbf{x}| = 1 \tag{5}$$

This is what is called "template matching." But in addition to this, we may also want a minimum similarity to exist between the input and its most similar pattern, that is

(6) $$s_i \geq \rho_i = 1 - \frac{r_i^2}{2}$$

where
ρ_i = the vigilance parameter
r_i = called the radius of similarity.

The domain of class C_i is therefore a hypersphere with center $\mathbf{w}_i$ and radius $\mathbf{r}_i$. The simultaneous use of the two above conditions with classes C_i, with different patterns $\mathbf{w}_i$ and radius of similarity r_i can be implemented using the variable u_i:

(7) $$x \in C_i \Leftrightarrow u_i > u_j \forall j \neq i$$

where

(8) $$u_i = \mathbf{x}^t \mathbf{w}_i - \rho_i$$

(9) $$\rho_i = 1 - \frac{r_i^2}{2}$$

The network that implements this classification is the "winner takes all" of Figure 3.

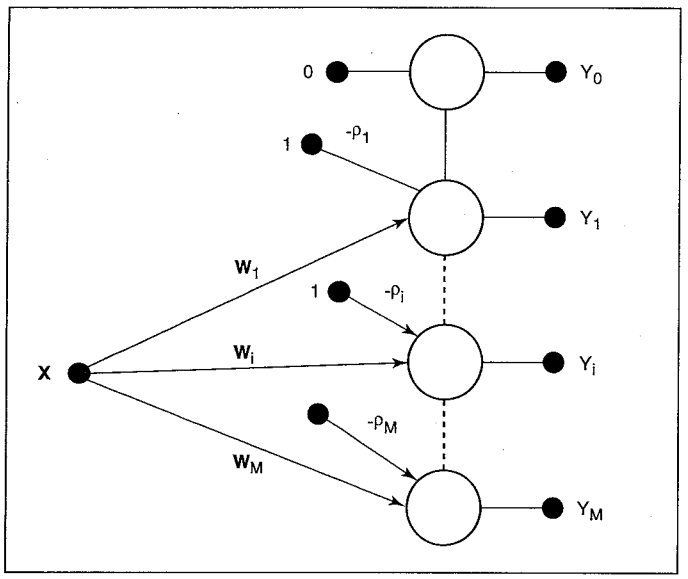

Figure 3 — Structure of the adaptive resonance theory (ART) network implemented (Haykin, 1994).

The winning neuron is the pattern most similar to the input that satisfies the minimum similarity condition. In case the neuron y_0 wins, no existing pattern satisfies the minimum similarity condition.

Figure 1a presents the center of the classes and their domain, as established by the network. In the case of classes with overlapping, the separator in the region belonging to both similarity hyperspheres (circles in this example) is the hyperplane (straight line in this example) that contains the intersection of the two hyperspheres, as would be expected. In Figure 1b, a nonspherical class is represented by three patterns. An input that activates any of these three neurons belongs to the class.

Training the Modified ART Network

This kind of network, called a modified ART network, brings together concepts of the one-dimensional Kohonen's layer, Grossberg's ART 1 and 2 networks (Wasserman, 1989), and the counterpropagation networks of Hecht-Nielsen (Wasserman, 1989). The training is called *semisupervised* because initially an ART network is trained for each class independently for different similarity radii.

Each of these networks is said to be specialized in its class. The training of the ART networks uses two alternative steps. If a neuron y_i is the winner, the input falls within the sphere of similarity of that neuron i, and its synapse vector undergoes a displacement in the direction of the input:

(10) $$\Delta \mathbf{w}_i = \alpha(\mathbf{x} - \mathbf{w}_i)$$

where
the training step α is typically 0.1.

This operation aims to lead pattern $\mathbf{w}_i$ toward the mean of the input it represents. If neuron y_0 is the winner, that means that no existing pattern represents the input with minimum similarity, and it is necessary to create a new pattern. A new neuron is then created with synapse vector $\mathbf{w}_{M+1} = \mathbf{x}$. The stopping criterion of the training must be defined previously; it is most common to establish the stop after a given number of steps without creating new patterns. After the training, all the patterns $\mathbf{w}_i$ found must have their modulus normalized for 1. The fact that $|\mathbf{x}| = 1$ does not imply that $|\mathbf{w}| = 1$.

An important matter in this kind of network is the equilibrium between the size of the radius of similarity and the number of patterns, because a radius of similarity that is too large may not discriminate between different classes, and creating many patterns implies an indefinition among the classes involved.

Therefore, for each class several specialist ART networks are trained, each with a different vigilance parameter, ρ, $\rho = 1 - r^2 / 2$, particularly with those obtained with r around r_{min} given by Equation 1. Each network has a different number N of patterns. That is the criticism of the different clustering (different networks) obtained depending on the section to be followed.

Quality of the Grouping of Each Class

An optimum grouping must present a minimum intraclass dissimilarity and maximum interclass dissimilarity (Duda et al., 2001). The intraclass dissimilarity, for a class C_j, can be measured by

(11) $$D_j^2 = \frac{1}{N_j} \sum_{\forall x \in C_j} |\mathbf{x} - \mathbf{w}_j|^2$$

and total intraclass dissimilarity, to be minimized, can be represented by

(12) $$D_{intra}{}^2 = \sum_{\forall j} N_j D_j^2 = \sum_{\forall j} \sum_{\forall x \in C_j} |\mathbf{x} - \mathbf{w}_j|^2$$

On the other hand, the clustering must be such that it maximizes interclass dissimilarity, which can be measured by:

(13) $$D_{inter}^2 = \sum_{\forall j} N_j |\mathbf{w}_j - \mathbf{w}_0|^2$$

where
$\mathbf{w}_0$ = the baricenter of all the inputs:

(14) $$\mathbf{w}_0 = \frac{1}{N} \sum_{\forall x} \mathbf{x}$$

Optimizing two objective functions is usually complicated. Fortunately, in our case it is possible to show that a sum of D^2_{inter} + D^2_{inter} is constant (Duda et al., 2001), that is, if we minimize D^2 we would automatically maximize D^2_{out}.

Let us consider the minimization of D^2. As we increase the number N of patterns $\mathbf{w}$ used in the clustering, D^2 decreases, but the patterns become nonrepresentative. Starting with one pattern, $N = 1$, for every pattern increase D^2 decreases, at first significantly and then in small steps. It is usually accepted that the largest N that still produces a significant decrease is the one that corresponds to a good "natural" clustering (Duda et al., 2001). Since the number of

patterns depends on the radius of similarity chosen, this is a second criterion for determining the radius of similarity.

The inflection point of D indicates only the region around which the optimum number of clusters must be, but the choice of N, the number of patterns of classes, needs to be complemented by a phenomenological or numerical analysis. The reason for this is that a region with a high population can present a considerable drop of D if it is represented by two quite similar patterns, and a low population region can be using a single pattern to represent rather unsimilar inputs. Phenomenologically, the first case can be evidenced by very similar patterns and the second by strange, unexpected patterns as a result of only the mean of two patterns and without physical meaning (Duda et al., 2001).

Numerically, the problem can be analyzed calculating a population N_i served by each pattern $\mathbf{w}_i$, that is, the inputs $\mathbf{x}$ for which $\mathbf{w}_i$ is the winning pattern and the value of D_i^2 for that population, given by

$$D_i^2 = \frac{1}{N_i} \sum_{\forall \mathbf{x} \in C_{w_i}} |\mathbf{x} - \mathbf{w}_i|^2 \quad (15)$$

where

C_{wi} = the set of vectors $\mathbf{x}$ such that $\mathbf{w}_i$ is the winning neuron.

The calculation of the mean of the distances between the various patterns $\mathbf{w}_i$, $p(d_{ij}, \forall i \neq j)$, where $d_{ij} = |\mathbf{w}_i - \mathbf{w}_j|^{0.5}$, also supplies essential information (Duda et al., 2001).

Two patterns $\mathbf{w}_i$ and $\mathbf{w}_j$ whose distance d_{ij} is considerably less than the mean and whose D_i^2 and D_j^2 are also considerably smaller than the mean, are strong candidates to be compacted into a single pattern.

A pattern $\mathbf{w}_k$ with a low population N_k and a high D_k^2 is a candidate to be partitioned into two or more different patterns. The result of the analysis of the quality of the clusters is the choice of the ART network that will represent each class. This kind of critical analysis of the clusters was made in this work.

Complete Neural Network

For every specialist network in each class, the neurons that represent the different class patterns have their outputs connected to a neuron of a nearby layer that implements a logical "or" and whose output indicates the relevance of the input to the class. In Figure 4, class 1 is made of patterns $\mathbf{w}_1$ through $\mathbf{w}_5$, class 2 of patterns $\mathbf{w}_6$ through $\mathbf{w}_9$, and class 3 of patterns $\mathbf{w}_{10}$ through $\mathbf{w}_{11}$. All the specialist networks are therefore connected in a single "winner takes all" (Wasserman, 1989).

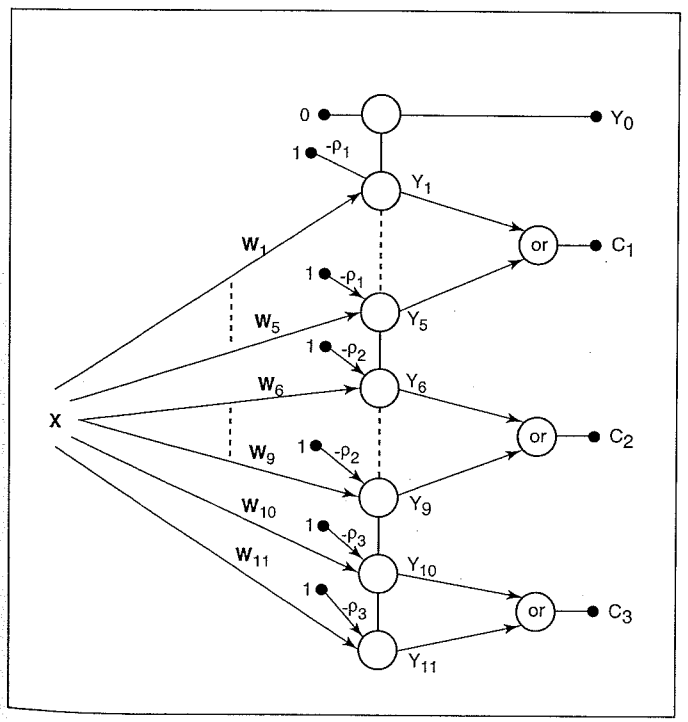

Figure 4 — Scheme of the complete modified ART network.

In the complete network, an active C_j outlet indicates that the input belongs to class C_j and an active y_0 outlet indicates that the input does not present sufficient similarity with any of the established patterns. If neuron y_0 is eliminated, the network will still present a classification; this is similar to the reclassification process that we use in the backpropagation networks (Part I). In this case, the indicated class is that which contains the pattern whose surface of the hypersphere of minimum similarity is closest to the input. Once the final network has been obtained, it must be tested with the training and testing sets.

Wrong classifications are called "invasions," because they mean that a pattern, with its sphere of similarity, invaded the domain of another class. To correct the problem, the radius of similarity of the neuron responsible for the wrong classification must be reduced until the classification is right. This implies, therefore, a recomposition of the specialist network that contained the neuron because its domain was reduced; it may be necessary to include new patterns so that it continues to reach the domain of its class. A large number of erroneous classifications may require correcting the networks.

RESULTS

Obtaining the Class Patterns

It should be noted that the profiles used will be subjected to the same preprocessing for amplitude normalization, noise softening and interpolation as the work done with the supervised networks described in the first paper, with the same number of points (276), and for this work the training and testing sets were formed by 100 profiles for each class: no discontinuity, porosity, longitudinal crack, slag inclusion, lack of fusion, lack of penetration and undercutting.

The first step in the process of clustering each class is to determine the radius of similarity and then the number of patterns to be used. As described above, there are two criteria: the first aimed primarily at the definition of the class domain, and the second trying to generate "natural" patterns for the classes. Since the objective of using clusters was mainly to generate patterns for the classes, the second technique was used. Since the number of "natural" patterns for each class must be quite limited, it started with a large radius of similarity in order to generate a single pattern, and then it was reduced gradually to generate a greater number of patterns, N. In this way the class patterns were obtained individually for each class of discontinuity: undercutting, lack of penetration, lack of fusion, porosity, slag inclusion and longitudinal crack, and for the class of "no discontinuity," by means of a processing routine in which the sets are inserted and the vigilance parameter is increased in fixed increments in order to increase the number of patterns created. Then the relation between the demerit factor D of the clusters of each class versus the number of patterns formed was studied, looking for the inflection point of the curve that characterizes the "natural" clustering. To visualize this relation, the graphs of N (number of patterns) versus D (demerit factor) were drawn. Figure 5 shows the graphs obtained for each class of weld discontinuity studied.

Analysis of the $N \times D$ graphs leads to the possible inflection points presented in Table 1 (arrows in Figure 5). These points are

Table 1 Possible inflection points (N) for each class analyzed

Class	Number of Patterns
No discontinuity	3
Porosity	2 and 9
Crack	4
Slag inclusion	2 and 5
Lack of fusion	2 and 4
Lack of penetration	2 and 7
Undercutting	2 and 3

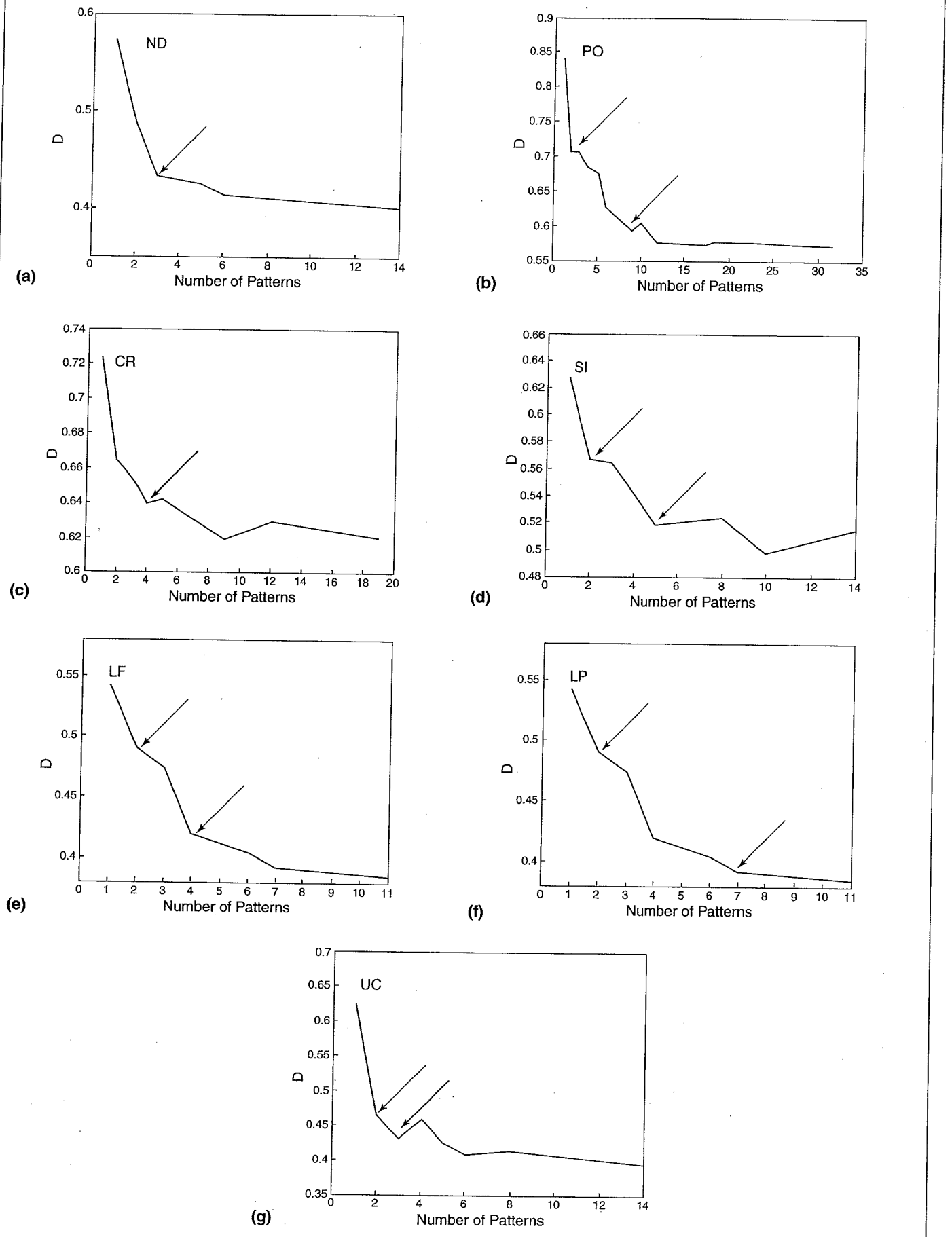

Figure 5 — Graphs of the number of patterns versus D *(demerit factor) for the various classes: (a) no discontinuity; (b) porosity; (c) longitudinal crack; (d) slag inclusion; (e) lack of fusion; (f) lack of penetration; (g) undercutting. The arrows show the probable inflection points.*

not absolute in the decision about the number of patterns representative of each class, but they define a study region.

The patterns generated for each of these cases are shown in Figures 6 through 10. For the similarity and individuality of the patterns to be appreciated, the figures are shown containing all the patterns found for each class of each N of Table 1. In the phenomenological analysis (Part III of this paper), the patterns adopted separately will be shown.

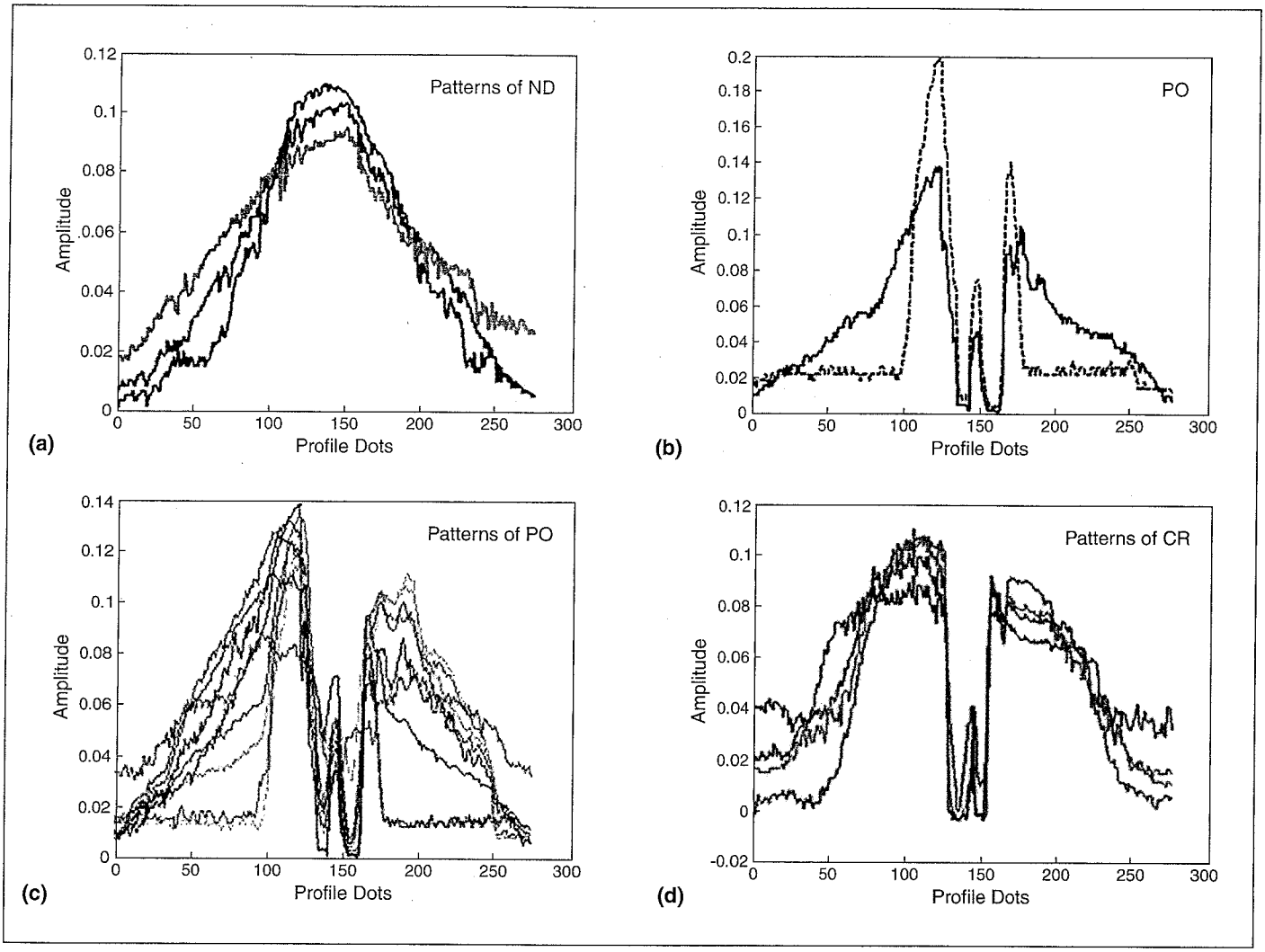

Figure 6 — Patterns generated for: (a) no discontinuity with $\rho = 0.56$ *and* $N = 3$*; (b) porosity with* $\rho = 0.22$ *and* $N = 2$*; (c) porosity with* $\rho = 0.43$ *and* $N = 9$*; (d) longitudinal crack with* $\rho = 0.55$ *and* $N = 4$.

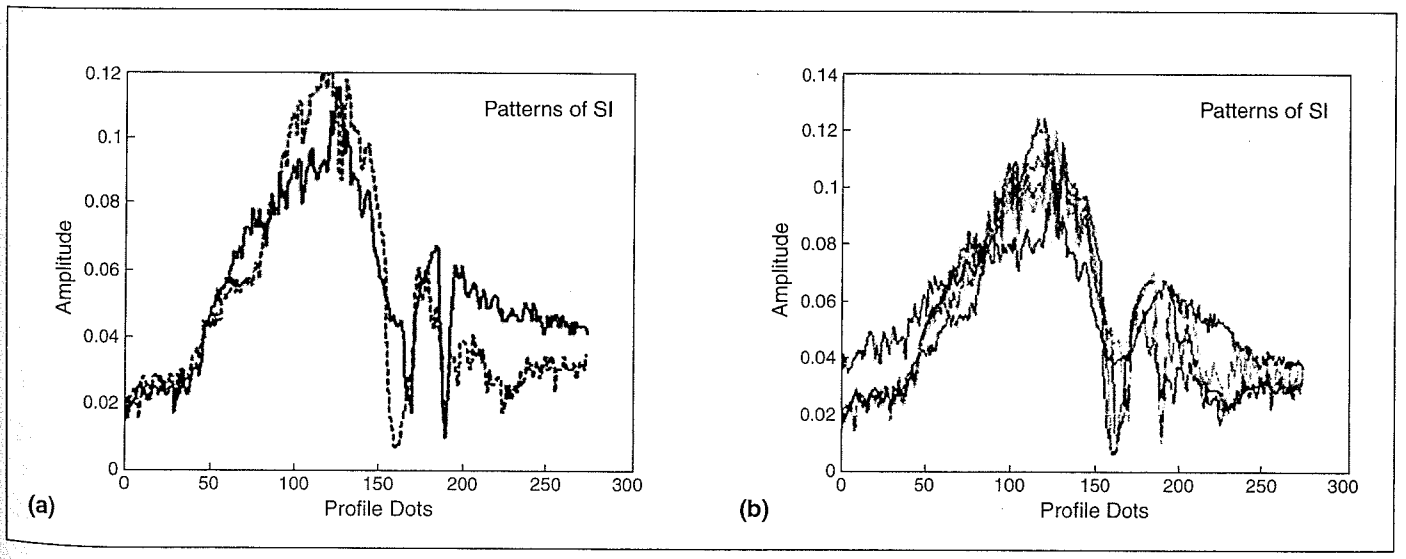

Figure 7 — Patterns generated for: (a) slag inclusion with $\rho = 0.45$ *and* $N = 2$*; (b) slag inclusion with* $\rho = 0.50$ *and* $N = 5$.

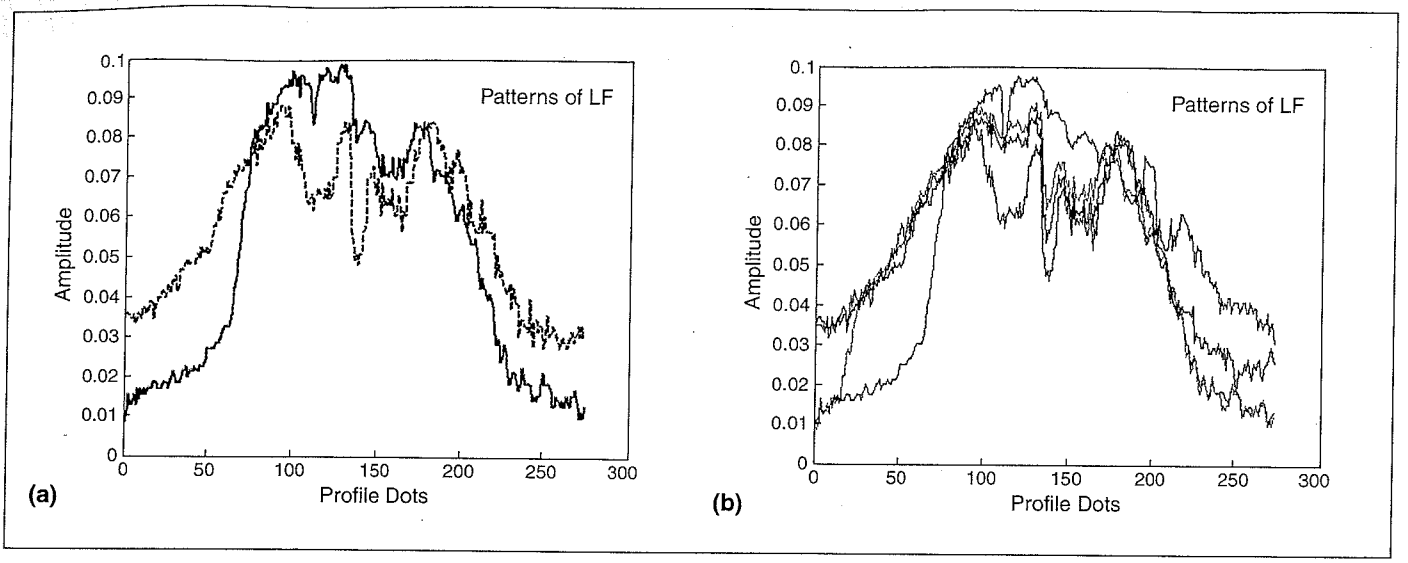

Figure 8 — Patterns generated for: (a) lack of fusion with ρ = 0.66 and N = 2; (b) lack of fusion with ρ = 0.74 and N = 4.

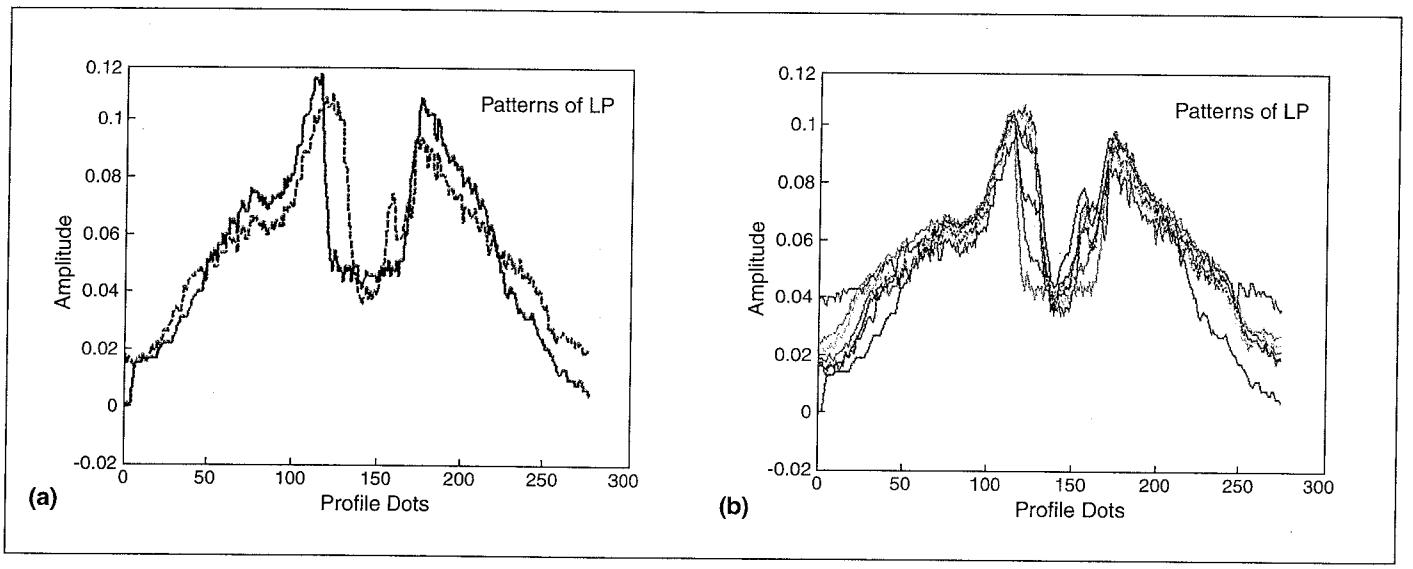

Figure 9 — Patterns generated for: (a) lack of penetration with ρ = 0.53 and N = 2; (b) lack of penetration with ρ = 0.63 and N = 7.

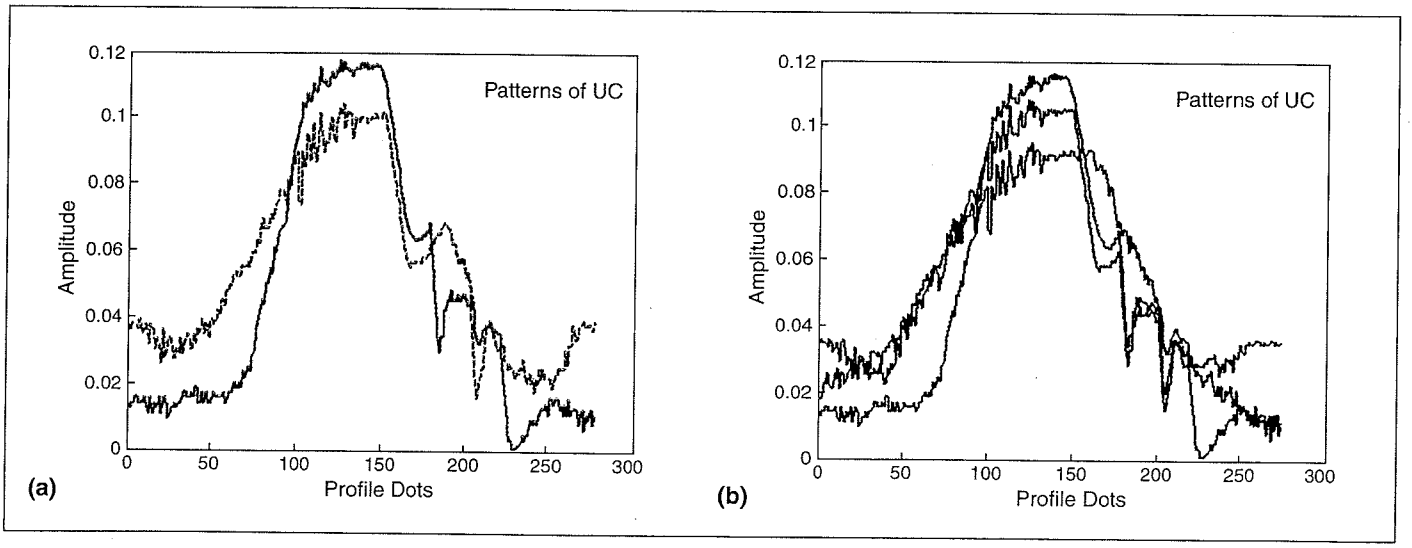

Figure 10 — Patterns generated for: (a) undercut with ρ = 0.60 and N = 2; (b) undercut with ρ = 0.63 and N = 3.

ACKNOWLEDGMENTS

The authors wish to acknowledge the National Council for Scientific and Technological Development, CAPES (Higher Level Training Agency) and FAPERJ (Research Foundation from Rio de Janeiro). The authors also thank the International Institute of Welding and Bundesanstalt für Materialforschung und -prüfung, Berlin for permission to publish the radiographic patterns used in the present work.

This work has been partially supported by a grant from the School of Engineering at Pontificia Universidad Católica de Chile.

REFERENCES

da Silva, R.R. and D. Mery, "The State of the Art of Weld Seam Radiographic Testing: Part I, Image Processing," *Materials Evaluation*, Vol. 65, 2007, pp. 643–647.

da Silva, R.R. and D. Mery, "The State of the Art of Weld Seam Radiographic Testing: Part II, Pattern Recognition," *Materials Evaluation*, Vol. 65, 2007, pp. 833–838.

da Silva, R.R., M.H.S. Siqueira, L.P. Calôba and J.M.A. Rebello, "Evaluation of the Relevant Feature Parameters of Welding Defects and Probability of Correct Classification Using Linear Classifiers," *Insight*, Vol. 44, 2002, pp. 616–622.

da Silva, R.R., M.H.S. Siqueira, L.P. Calôba and J.M.A. Rebello, "Pattern Recognition of Weld Defects Detected by Radiographic Test," *NDT&E International*, Vol. 37, 2004, pp. 461–470.

da Silva, R.R., M.H.S. Siqueira, L.P. Calôba and J.M.A. Rebello, "Estimated Accuracy of Classification of Defects Detected in Welded Joints by Radiographic Tests," *NDT&E International*, Vol. 38, 2005, pp. 335–348.

da Silva, R.R., M.H.S. Siqueira, L.P. Calôba and J.M.A. Rebello, "Radiographics Pattern Recognition of Welding Defects Using Linear Classifiers," *Insight*, Vol. 43, 2001, pp. 669–674.

de Pádua, G.X., R.R. Silva, J.M.A. Rebello and L.P. Calôba, "Classification of Welding Defects in X-rays Using Transverse Profiles to the Weld Seam," *16th World Conference on Nondestructive Testing Book of Abstracts*, Montreal, ICNDT, 2004, pp. 90–91.

Duda, R.O., P.E. Hart and D.G. Stork, *Pattern Classification*, second edition, New York, Wiley, 2001.

Felisberto, M.K., H.S. Lopes, T.M. Centeno and L.V.R. Arruda, "An Object Detection and Recognition System for Weld Bead Extraction from Digital Radiographs," *Computer Vision and Image Understanding*, Vol. 102, No. 3, 2006, pp. 238–249.

Fücsök, F., C. Mueller and M. Scharmach, "Reliability of Routine Radiographic Film Evaluation — An Extended ROC Study of the Human Factor," *8th ECNDT Abstracts Book*, Madrid, Spanish Society for NDT, 2002, p. 439.

Fücsök, F., C. Müller and M. Scharmach, "Human Factors: The NDE Reliability of Routine Radiographic Film Evaluation," *15th World Conference on Non-destructive Testing*, Rome, AIPnD, 2000, p. 758.

Halmshaw, R., *Industrial Radiology: Theory and Practice*, London, Chapman and Hall, 1995.

Haykin, S., *Neural Networks — A Comprehensive Foundation*, New York, Macmillian, 1994.

Liao, T.W. and Y. Li, "An Automated Radiographic NDT System for Weld Inspection: Part II — Flaw Detection," *NDT&E International*, Vol. 31, No. 3, 1998, pp. 183–192.

Liao, T.W. and J. Ni, "An Automated Radiographic NDT System for Weld Inspection: Part I — Weld Extraction," *NDT&E International*, Vol. 29, No. 3, 1996, pp. 157–162.

Liao, T.W., D. Li and Y. Li, "Detection of Welding Flaws from Radiographic Images with Fuzzy Clustering Methods," *Fuzzy Sets and Systems*, Vol. 108, 1999, pp. 145–158.

Mery, D., "Automated Radioscopic Testing of Aluminium Die Castings," *Materials Evaluation*, Vol. 64, 2006, pp. 135–143.

Wasserman, P.D., *Neural Computing Theory and Practice*, New York, Coriolis Group, 1989.